

Raman, Infrared, and Ultraviolet Spectra of the Chlorine Difluoride Free Radical in Solid Nitrogen

ELEANOR S. PROCHASKA and LESTER ANDREWS*

Received July 8, 1976

AIC60490D

Matrix samples of chlorine monofluoride and fluorine were photolyzed by a mercury arc or argon ion laser, and a 578, 570 cm⁻¹ infrared doublet, a new 500-cm⁻¹ Raman band, and a new 320-nm ultraviolet absorption were observed and assigned to the ClF₂ free radical. The F-Cl-F valence angle lower limit is calculated to be 136 ± 4° from isotopic ν₃ assignments, while mutual exclusion was observed between the infrared and Raman spectra. The experimental data do not exclude a linear geometry, but a slightly bent radical is suggested.

Introduction

The chlorine difluoride free radical was first reported by Mamantov and co-workers¹ from the observation of a strong infrared doublet at 578 and 570 cm⁻¹ following the photolysis of ClF and F₂ in matrices. ClF₂ is of unique theoretical interest as a 21-electron molecule since its structure, which has not been definitively determined, might be bent like 20-electron molecules or linear like 22-electron species. In fact, simple molecular orbital theory² and SCF calculations³ have suggested that the orbital containing the free-radical electron attains minimum energy in the linear configuration, although the detailed calculations³ and an experimental estimate¹ place the F-Cl-F angle in the 140° range.

Since the Raman spectrum is valuable for structure determination of symmetrical triatomics, the Raman spectrum of ClF₂ was sought using laser photolysis techniques developed in a matrix-Raman study of the OF free radical.⁴ Infrared studies were also performed, and the optical spectrum of ClF₂ was obtained for comparison to theory.

Experimental Section

The cryogenic refrigeration systems and vacuum vessels used for infrared,^{5,6} Raman,⁴ and optical⁷ studies have been described previously. The stainless steel vacuum lines and sample cans were passivated with several inches of ClF or ClF₃ (Ozark-Mahoning) overnight before each use. Chlorine monofluoride was condensed at 77 K, degassed, and distilled from a *n*-pentane slush at -130 °C into the sample can. Fluorine (Matheson) and argon (Air Products, 99.998%) or nitrogen (Air Products, ultrahigh purity) were then added directly. Sample concentrations used in these studies for (N₂ or Ar)/F₂/ClF ranged from 200/1/2 to 200/2/1 in infrared and from 20/1/2 to 100/1/2 in Raman studies; deposition rates were about 2 mmol/h. Several Raman experiments were done with fluorine and chlorine (Matheson) samples; chlorine was condensed and degassed before use.

For the infrared and optical investigations, samples were subjected to photolysis using a BH-6 high-pressure mercury arc (General Electric) focused by a quartz lens system through a 5-cm saturated CoSO₄-NiSO₄ filter (passes 230-350 nm). Infrared spectra were recorded from 200 to 1600 cm⁻¹ on a Beckman IR-12 spectrophotometer and optical spectra were taken on a Cary 17 instrument in the 2000-200-nm range. Raman spectra were recorded on a Spex Ramalog using argon and krypton plasma lasers (Coherent Radiation) and calibrated against plasma emission lines.

Results

Infrared, Raman, and ultraviolet studies of chlorine monofluoride-fluorine matrix systems will be described in turn.

Infrared Data. Several infrared experiments were performed with N₂/F₂/ClF = 200/1/2 and 200/2/1 samples; spectra from the 200/2/1 experiment are illustrated in Figure 1. Trace (a) was recorded after depositing 49 mmol of sample over a 24-h period; a very strong well-resolved ClF doublet was observed at 764.0 and 757.0 cm⁻¹; a weak doublet at 723 and 710 cm⁻¹ presumably due to FClO₃ impurity⁸ and two weak doublets at 617, 609 cm⁻¹ and 545, 541 cm⁻¹ due to FClO₂ impurity⁹ were observed in the original spectrum. After

mercury-arc photolysis for two periods of 20 min, scan (b) was taken. Note the appearance of a strong well-resolved doublet at 578 and 570 cm⁻¹ (0.40 and 0.13 OD), which has been assigned to the ClF₂ radical,¹ ClF₃ bands¹⁰ at 679 and 668 cm⁻¹ (0.11 and 0.12 OD), and a weak feature at 631 cm⁻¹. Following temperature cycling of the sample from 14 to 21 to 14 K, spectrum (c) was recorded, which shows a marked growth of the 578, 570 cm⁻¹ doublet (1.0, 0.30 OD) without changes in the other spectral features, except the slight sharpening of a weak, broad band (0.01 OD) near 242 cm⁻¹. No new absorptions were observed in the 400-540-cm⁻¹ region. Continued photolysis of the sample decreased the 578, 570 cm⁻¹ doublet, as reported previously.¹ The inset trace (d) shows an expanded-scale scan of the new doublet after photolysis but before temperature cycling. The doublet was recorded ten times in two experiments at 577.6 ± 0.1 and 570.0 ± 0.1 cm⁻¹, and the chlorine isotopic splitting of 7.6 ± 0.1 cm⁻¹ was measured directly from the chart paper. This splitting is in agreement with the earlier value;¹ however, the present band contour was sufficiently symmetric to allow direct measurement without curve analysis.

A similar argon matrix experiment was done with an Ar/F₂/ClF = 200/1/2 sample. The ClF doublet at 770, 763 cm⁻¹ exhibited a site splitting⁹ at 767, 760 cm⁻¹. Photolysis for 2 h produced ClF₃ bands¹⁰ at 684, 673 cm⁻¹, a weak, sharp doublet at 636, 627 cm⁻¹, and a new 574-cm⁻¹ band (0.27 OD) with asymmetry on the low frequency side. Cycling the sample to 23 K made the 574-cm⁻¹ absorption completely absorbing and produced a weak new band at 536 cm⁻¹ along with broad features at 620 and 665 cm⁻¹.

Raman Data. After several Raman experiments using N₂/F₂/ClF = 100/1/2 samples gave only a weak ClF signal near 760 cm⁻¹ and no product bands, a 20/1/2 sample was deposited in part to thoroughly passivate all of the spray-on line. The initial Raman spectrum, using 110 mW of 530.9-nm excitation at the sample, showed a strong doublet at 762 and 752 cm⁻¹, a weak F₂ band⁴ at 890 cm⁻¹, and a weak triplet at 550, 524, and 500 cm⁻¹. Subsequent scans over a 30-min period doubled the 524- and 500-cm⁻¹ signals relative to the 550-cm⁻¹ band, which is due to matrix-isolated chlorine.¹¹ A scan with 647.1-nm excitation on a new sample area revealed the same Raman signals with reduced intensity. When 600 mW of 488.0-nm excitation was used, a tenfold increase in Raman signals at 890, 760, 550, 524, and 500 cm⁻¹ resulted. Again, after 30 min of exposure to the laser beam, the 524- and 500-cm⁻¹ signals doubled relative to the 550-cm⁻¹ signal. The same Raman-shifted bands were observed with slightly reduced intensities using 476.5- and 457.9-nm excitation.

Three more Raman experiments were performed with the ClF-F₂ system and the spectra are shown in Figure 2. The first scan (a) after exposure of a N₂/F₂/ClF = 50/1/2 sample to 600 mW of 488.0-nm radiation shows a grating ghost at 951 cm⁻¹, F₂ at 890 cm⁻¹, ClF at 760 cm⁻¹, Cl₂ at 550 cm⁻¹, and a ClF₃ signal¹² at 524 cm⁻¹. The dramatic effect of sample

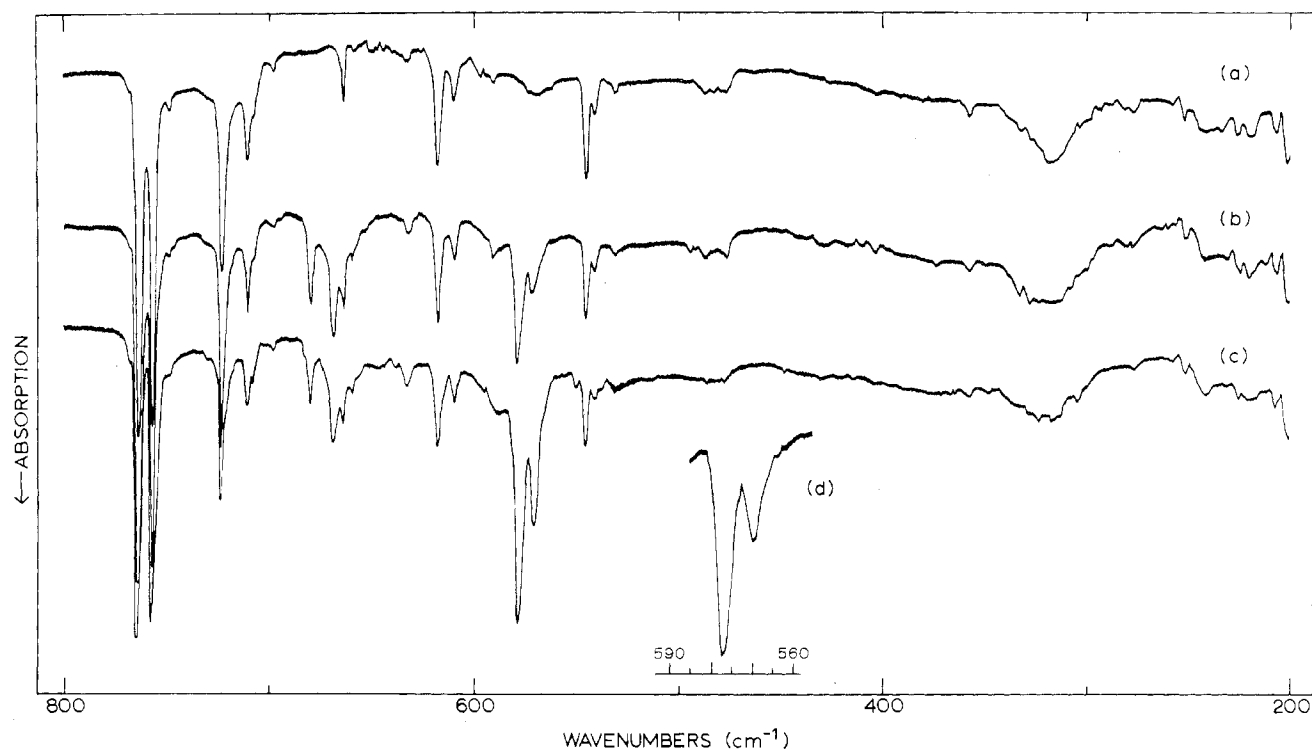


Figure 1. Infrared spectra in the 200–800- cm^{-1} region for a $\text{N}_2/\text{F}_2/\text{ClF} = 200/2/1$ sample. Spectrum (a) is for sample deposited at 14 K for 22 h, (b) was recorded after 20-min photolysis, and (c) followed a temperature cycle to 21 K. Spectrum (d) is an expanded-scale scan of the new doublet in spectrum (b). The sharp, weak bands in the 200–300- cm^{-1} region are due to incomplete purge of water vapor in the instrument.

exposure to 60 min of laser photolysis is shown in trace (b); the F_2 and ClF signals were reduced, and the Cl_2 signal remained unchanged, while the 524- cm^{-1} ClF_3 band increased fourfold and a very strong new signal appeared at 500 cm^{-1} . Figure 2(c) contrasts a 514.5-nm excitation spectrum of a $\text{N}_2/\text{F}_2/\text{ClF} = 100/1/2$ sample after a 60-min exposure to the 488.0-nm laser; the grating ghost shifted to 900 cm^{-1} and the same Raman signals were observed. Finally, the 457.9-nm excited Raman spectrum of an $\text{Ar}/\text{F}_2/\text{ClF} = 50/1/2$ sample after 60 min of 488.0-nm photolysis is shown in Figure 2(d). The F_2 and ClF signals were reduced and the ClF_3 and new 500- cm^{-1} bands were increased by prolonged exposure to the laser beam.

Several of the above Raman studies employed mercury-arc photolysis, but this technique was not as effective for producing new signals as photolysis by the laser beam. Also, a 12 to 21 to 12 K thermal cycle of a sample previously irradiated by 488.0-nm light caused a slight decrease in scattered light intensity without any relative change in the Raman signals.

Complementary Raman experiments were performed on the chlorine-fluorine system using 100/1/1 and 50/1/1 samples of F_2 and Cl_2 in argon and nitrogen matrices. Spectra from the $\text{N}_2/\text{F}_2/\text{Cl}_2 = 50/1/1$ experiment are shown in figure 3. The first scan (a) using 450 mW of 488.0-nm excitation at the sample gave a full-scale Cl_2 band at 550 cm^{-1} with a shoulder at 525 cm^{-1} due to ClF_3 , no signal at 490–510 cm^{-1} , and sharp medium-intensity bands at 760 cm^{-1} due to ClF and at 890 cm^{-1} due to F_2 . After 20 min of additional exposure to the laser beam, the spectrum shown in Figure 3(b) was recorded. A sharp new band appeared at 500 ± 2 cm^{-1} , a strong composite ClF_3 - Cl_2 band at 525–550 cm^{-1} , a ClF_3 band at 752 cm^{-1} with a 760- cm^{-1} ClF shoulder, and a weak F_2 band at 890 cm^{-1} . The analogous argon matrix experiments gave a threefold increase in the ClF band at 760 cm^{-1} on the initial scan. Following a 20-min laser photolysis period, the growth of ClF_3 was indicated by strong new signals at 525 and 750 cm^{-1} and a weak band at 435 cm^{-1} ; weak (10%) new signals

also appeared at 500 and 635 cm^{-1} .

A $\text{N}_2/\text{ClF}_3 = 50/1$ sample was investigated using 488.0- and 514.5-nm excitation. Chlorine trifluoride Raman bands¹² were observed at 752 cm^{-1} (relative intensity 30), 524 cm^{-1} (100), and 430 cm^{-1} (6). Exposure to 900 mW of 488.0-nm light halved the ClF_3 band intensity without producing any new signals, although the strong 524- cm^{-1} signal would obscure a weak Raman band at 500 cm^{-1} .

Ultraviolet Data. Several optical studies were done on the chlorine fluoride matrix system. An $\text{Ar}/\text{F}_2/\text{ClF} = 200/1/2$ sample was studied in the ultraviolet region, and the spectra are shown in Figure 4. After deposition of 9 mmol of sample for 5 h at 25 K, spectrum (a) revealed a weak, broad ClF absorption near 270 nm. Photolysis for a total of 75 min produced a weak, broad new band at 320 nm (0.04 OD), which is shown in Figure 4(b). A scan through the near-infrared from 2000 to 450 nm revealed no absorptions. After rapid temperature cycles to 40 and 45 K, the new band increased to 0.25 OD, Figure 4(c). A similar nitrogen matrix experiment also produced a 320-nm absorption following photolysis and temperature cycling. As in infrared experiments, further photolysis markedly reduced the new band, but another temperature cycle restored the new absorption.

A sample of $\text{Ar}/\text{ClF}_3 = 100/1$ was also investigated. Figure 4(d) shows the spectrum of 5 mmol of sample deposited at 25 K. The absence of absorption maxima in the near-ultraviolet is consistent with the absorption spectrum of ClF_3 gas.¹³ Photolysis for two 20-min periods produced a broad weak absorption at 320 nm, Figure 4(e), which was markedly increased by temperature cycles to 40 and 45 K, Figure 4(f). Twenty more minutes of photolysis essentially destroyed the new 320-nm absorption, Figure 4(g); however, another 45-K temperature cycle restored the new band, Figure 4(h).

Finally, an $\text{Ar}/\text{FClO}_3 = 100/1$ sample was subjected to the same experimental treatment. Photolysis and temperature cycling produced an increased spectral background, but no new absorption bands were observed.

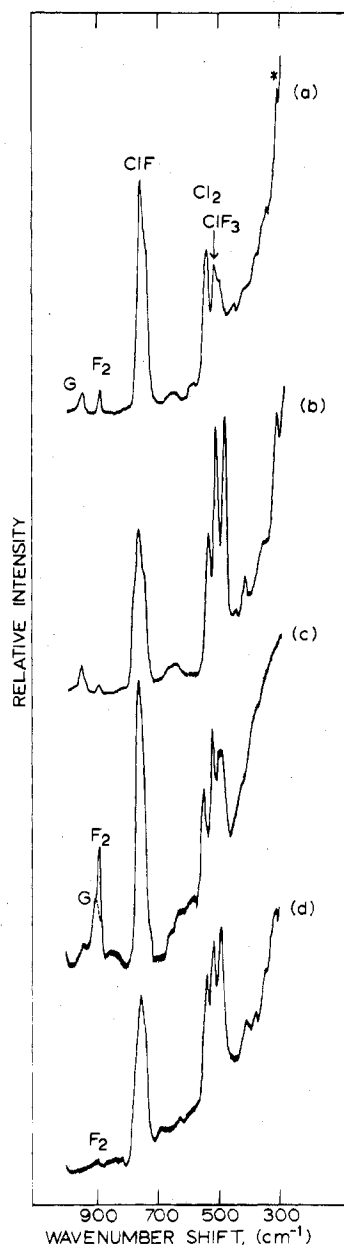


Figure 2. Raman spectra of matrix samples of fluorine and chlorine monofluoride. Spectrum (a) is for the $\text{N}_2/\text{F}_2/\text{ClF} = 50/1/2$ sample; the original spectrum was scanned on 3×10^{-9} Å range at $50 \text{ cm}^{-1}/\text{min}$ using 600 mW of 488.0-nm excitation at the sample, which was exposed to the laser beam for 6 min when 500 cm^{-1} was scanned. Spectrum (b) is the same as (a) following sample exposure to a laser beam for 60 min. Spectrum (c) is for the $\text{N}_2/\text{F}_2/\text{ClF} = 100/1/2$ sample after exposure to a 488.0-nm laser beam for 60 min, recorded with 700 mW of 514.5-nm excitation on a 0.3×10^{-9} Å range. Spectrum (d) is for the $\text{Ar}/\text{F}_2/\text{ClF} = 50/1/2$ sample after exposure to a 488.0-nm beam for 60 min, recorded with 100 mW of 457.9-nm excitation on a 1×10^{-9} Å range. The asterisk denotes a laser plasma emission line, and G denotes a grating ghost.

Discussion

The vibrational and electronic transition assignments, molecular geometry, and bonding for ClF_2 will be discussed.

Vibrational Assignments. The Mamantov paper on ClF_2 presented convincing evidence for assignment of the 578, 570 cm^{-1} doublet to ν_3 of $^{35}\text{ClF}_2$ and $^{37}\text{ClF}_2$, and the present observations support that finding. However, the case for assigning the very weak 242-cm^{-1} band to ν_2 is not nearly as strong, and on the basis of the present observation of only a very weak, broad 242-cm^{-1} band, the ν_2 assignment must be considered tentative.

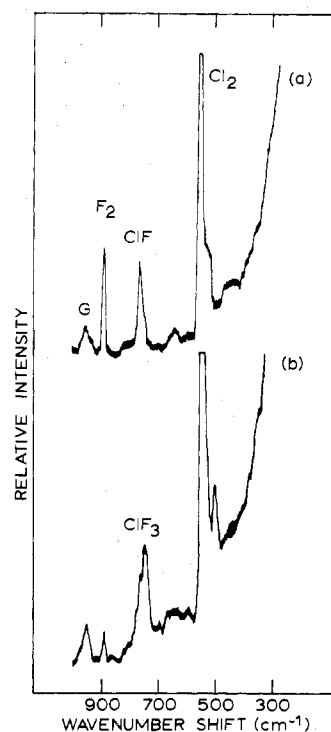


Figure 3. Raman spectra of matrix samples of fluorine and chlorine. Spectrum (a) is for the $\text{N}_2/\text{F}_2/\text{Cl}_2 = 50/1/1$ sample. The original spectrum was scanned on a 0.3×10^{-9} Å range at $50 \text{ cm}^{-1}/\text{min}$ using 450 mW of 488.0-nm excitation at the sample, which was exposed to the laser beam for 6 min when 500 cm^{-1} was scanned. Spectrum (b) is the same as (a) following sample exposure to a laser beam for 30 min.

Of more significance is the symmetric stretching mode, ν_1 . The Mamantov study assigned a weak 536-cm^{-1} infrared band to ν_1 of ClF_2 . Although a 536-cm^{-1} band was observed in the present argon matrix work following sample warming, no $480\text{--}540\text{-cm}^{-1}$ absorption was observed in the present nitrogen matrix experiments, even when the $578, 570 \text{ cm}^{-1}$ doublet was very strong. Accordingly, the infrared observation of ν_1 of ClF_2 must be questioned.

The Raman studies of argon and nitrogen matrix samples of ClF and F_2 revealed a strong new 500-cm^{-1} Raman band which is appropriate for ClF_2 . First, laser photolysis of matrix-isolated OF_2 produced a steady growth of Raman signal for the OF free radical which requires the photodissociation of OF_2 with the diffusion of F atoms away from the site of their production.⁴ The present Raman spectra show that F_2 and ClF are consumed as a function of laser exposure time while the most intense Raman band of ClF_3 increases and a strong, new 500-cm^{-1} Raman band appears. The new 500-cm^{-1} band is attributed to ClF_2 produced by the reaction of ClF with F atoms from laser photodissociation of molecular fluorine. In the $\text{N}_2/\text{F}_2/\text{Cl}_2$ Raman experiments, ClF , ClF_3 , and the 500-cm^{-1} bands grow with laser exposure time, which also supports assignment of the new 500-cm^{-1} band to ClF_2 . Second, the ν_1 mode of ClF_2 at 500 cm^{-1} is in accord with ν_1 of ClF_2^- at 476 cm^{-1} ¹⁴ and ν_1 of XeF_2 and KrF_2 at 512 and 452 cm^{-1} , respectively.¹⁵ Accordingly, the 500-cm^{-1} Raman band is assigned to ν_1 of the ClF_2 radical.

The 636-cm^{-1} infrared band has been observed strongly in experiments photolyzing mixtures of Cl_2 and F_2 in solid argon,^{16,17} and evidence for its assignment to Cl_2F_2 has been presented.¹⁶ Similar Br_2 and F_2 experiments support this assignment, as will be described in a later publication.

Electronic Transition. Similar optical absorption studies reveal a single new absorption at 320 nm which exhibits the same photolysis and temperature cycling behavior as the $578,$

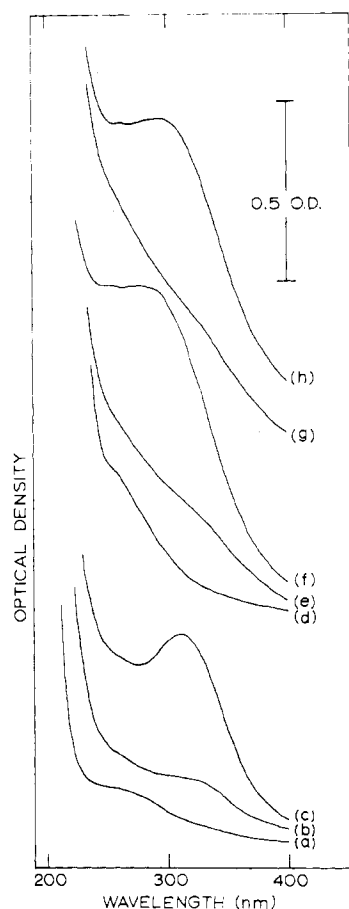


Figure 4. Ultraviolet spectra of chlorine fluoride matrix samples. Spectrum (a) is for the $\text{Ar}/\text{F}_2/\text{ClF} = 200/1/2$ sample deposited for 4 h, trace (b) followed 75 min of photolysis, and scan (c) was recorded after temperature cycles to 40 and 45 K. Spectrum (d) is for the $\text{Ar}/\text{ClF}_3 = 100/1$ sample deposited for 4 h, trace (e) was recorded after photolysis for 40 min, and scan (f) followed temperature cycles to 40 and 45 K. Spectrum (g) shows the effect of 20 min of additional photolysis and scan (h) followed another temperature cycle to 45 K.

570 cm^{-1} infrared doublet. Since ClF_3 does not exhibit an absorption band in the near-ultraviolet, the 320-nm feature is assigned to ClF_2 .

The electronic absorption is assigned to a ${}^2\Sigma_g^+ \rightarrow {}^2\Sigma_u^+$ transition for ClF_2 . Following the orbital designation of Ungemach and Schaefer³ for a linear molecule, the orbital transition is $(4\sigma_u)^2 \dots (6\sigma_g) \rightarrow (4\sigma_u) \dots (6\sigma_g)^2$. The analogous ${}^2\Sigma_g^+ \rightarrow {}^2\Sigma_u^+$ transition for Cl_3^- has been observed at 250 nm.¹⁸ The ${}^2\Sigma_g^+ \rightarrow {}^2\Pi_u$ transition for ClF_2 has been predicted³ near 1 eV. No absorption was observed in the near-infrared; however, this transition is expected to be significantly weaker than the ultraviolet absorption.

Structure and Bonding. The structure of ClF_2 is of theoretical significance as it is the best documented 21-electron molecule. Two pieces of experimental evidence reflect on the structure of ClF_2 , the apex angle calculation from isotopic ν_3 frequencies and the comparison of infrared and Raman spectra. First, apex angle determinations from observed frequencies provide an upper or lower limit depending on terminal or apex isotopic substitution.¹⁹ In the case of ClF_2 , the angle calculated from the $7.6 \pm 0.1\text{ cm}^{-1}$ isotopic shift, $136 \pm 4^\circ$, is a lower limit. Calculations of this type are reliable for angles in the $100\text{--}120^\circ$ range where the cosine function changes rapidly and terminal and apex isotopic substitutions are available to average the results and minimize the effect of anharmonicity. The upper limit–lower limit average calculated from isotopic ν_3 frequencies for ozone is

Table I. Force Constants and Bond Lengths for Simple Chlorine–Fluorine Species

Species	F_r , mdyn/Å	F_{rr} , mdyn/Å	r , Å	Ref
ClF	4.24		1.63	a
ClF_2^+ (100 °C)	4.83	0.21	1.70	b
ClF_2 (150 °C)	2.48	0.13	1.83	c
ClF_2 (180 °C)	2.30	0.50	1.79	c
ClF_2^- (180 °C)	2.35	0.17	1.93	d

^a Force constants calculated from matrix data; bond length from B. Rosen, "Spectroscopic Constants", Pergamon Press, New York, N.Y., 1970. ^b Force constants calculated from data of R. J. Gillespie and M. J. Morton, *Inorg. Chem.*, 9, 616 (1970), using symmetry coordinates; bond length calculated in ref 3. ^c Force constants calculated from present data using symmetry coordinates; bond length from ref 3. ^d Force constants from ref 14; bond length from ref 3.

within 1° of the true angle.²⁰ However, the upper limit for ClF_2 cannot be determined and it must be presumed to be 180° . Accordingly, the apex angle calculation for ClF_2 suggests a nonlinear molecule with an angle of perhaps $150\text{--}160^\circ$, but it cannot eliminate the linear structure. In support of a nonlinear geometry for ClF_2 are the 125° lower limit for Cs_2O based on isotopic ν_3 frequencies²¹ and the electric deflection of Cs_2O which requires a dipole moment.²²

On the other hand, the mutual exclusion of ν_1 from the infrared and ν_3 from the Raman spectrum indicates a linear molecule, *within the limits* of detectability. It is, of course, possible for ClF_2 to be slightly bent where both stretching modes would be allowed in the infrared and Raman spectra, but the ν_3 infrared and ν_1 Raman intensities would very strongly dominate. Ozone is a bent molecule with very weak ν_1 infrared absorption and very weak ν_3 Raman intensity.²⁰

In conclusion, the experimental evidence does not definitively determine the nonlinearity of the ClF_2 radical, but it probably favors a slightly bent species, in agreement with recent SCF calculations.³

Table I summarizes Cl–F bond stretching force constant data relevant to bonding in chlorine–fluorine species. The ClF diatomic, of course, has a normal electron-pair bond. The 20-electron ClF_2^+ species has basically four net bonding electrons²³ which gives two single Cl–F bonds and a 4.83 mdyn/Å force constant, near the ClF diatomic value of 4.24 mdyn/Å. The 21st electron appears to be effectively anti-bonding from the dramatic decrease in force constant for ClF_2 radical to 2.48 mdyn/Å, although the effect of the 22nd electron is less in ClF_2^- with a 2.35 mdyn/Å force constant. The calculated bond lengths³ for these species increase as the force constants decrease.

Conclusions

Photolysis of matrix samples of ClF and F_2 produced an infrared doublet at 578, 570 cm^{-1} , a new 500-cm^{-1} Raman band, and an ultraviolet absorption at 320 nm which are attributed to the chlorine difluoride free radical. The apex angle lower limit determined from isotopic ν_3 frequencies is $136 \pm 4^\circ$ while mutual exclusion holds for ν_3 and ν_1 in the infrared and Raman spectra within the limits of detectability. Although the experimental evidence does not rule out a linear structure, a slightly bent species is favored.

Acknowledgment. The authors gratefully acknowledge support for this research by the National Science Foundation under Grant CHE-73-08686-A03 and the assistance of Dr. B. S. Ault with several experiments.

Registry No. ClF, 7790-89-8; ClF_2^+ , 32629-46-2; ClF_2 , 24801-48-7; ClF_3 , 7790-91-2; F_2 , 7782-41-4; Cl_2 , 7782-50-5.

References and Notes

- (1) G. Mamantov, E. J. Vasini, M. C. Moulton, D. G. Vickroy, and T. Maekawa, *J. Chem. Phys.*, 54, 3419 (1971).

- (2) G. C. Pimentel, *J. Chem. Phys.*, **19**, 446 (1951).
 (3) S. R. Ungemach and H. F. Schaefer, III, *J. Am. Chem. Soc.*, **98**, 1658 (1976).
 (4) L. Andrews, *J. Chem. Phys.*, **57**, 51 (1972).
 (5) L. Andrews, *J. Chem. Phys.*, **48**, 972 (1968).
 (6) L. Andrews, *J. Chem. Phys.*, **54**, 4935 (1971).
 (7) L. Andrews, *J. Chem. Phys.*, **63**, 4465 (1975).
 (8) D. R. Lide, Jr., and D. E. Mann, *J. Chem. Phys.*, **25**, 1128 (1956).
 (9) L. Andrews, F. K. Chi, and A. Arkell, *J. Am. Chem. Soc.*, **96**, 1997 (1974).
 (10) R. A. Frey, R. L. Reddington, and A. L. K. Aljibury, *J. Chem. Phys.*, **54**, 344 (1971).
 (11) B. S. Ault, W. F. Howard, Jr., and L. Andrews, *J. Mol. Spectrosc.*, **55**, 217 (1975).
 (12) H. Selig, H. H. Claassen, and J. H. Holloway, *J. Chem. Phys.*, **52**, 3517 (1970).
 (13) H. Schmitz and H. J. Schumacher, *Z. Naturforsch. A*, **2**, 363 (1947).
 (14) K. O. Christe, W. Sawodny, and J. P. Guertin, *Inorg. Chem.*, **6**, 1159 (1967).
 (15) W. F. Howard, Jr., and L. Andrews, *J. Am. Chem. Soc.*, **96**, 7864 (1974).
 (16) M. R. Clarke, W. H. Fletcher, G. Mamantov, E. J. Vasini, and D. G. Vickroy, *Inorg. Nucl. Chem. Lett.*, **8**, 611 (1972).
 (17) A. Arkell, L. M. Huber, and I. Schwager, Technical Report AFRPL-TR-67-69, Texaco, Inc., Beacon, NY., 1967.
 (18) L. Andrews, *J. Am. Chem. Soc.*, **98**, 2152 (1976).
 (19) M. Allavena, R. Rysnik, D. White, V. Calder, and D. E. Mann, *J. Chem. Phys.*, **50**, 3399 (1969).
 (20) L. Andrews and R. C. Spiker, Jr., *J. Phys. Chem.*, **76**, 3208 (1972).
 (21) R. C. Spiker, Jr., and L. Andrews, *J. Chem. Phys.*, **58**, 713 (1973).
 (22) A. Buchler, J. L. Stauffer, and W. Klemperer, *J. Chem. Phys.*, **46**, 605 (1966).
 (23) See for example H. B. Gray, "Electrons and Chemical Bonding", W. A. Benjamin, New York, N.Y., 1965, pp 99, 151.

Contribution from the Institute of Inorganic Chemistry,
University of Fribourg, 1700 Fribourg, Switzerland

Stability of Gaseous Complexes between Two- and Three-Valent Metal Halides

F. P. EMMENEGGER

Received January 15, 1976

AIC60041D

The formation of gaseous complexes according to $\text{MX}_2(\text{s}) + 2\text{LX}_3(\text{g}) = \text{ML}_2\text{X}_6(\text{g})$ was measured for the following compounds (in parentheses are mean temperature; method of investigation): $\text{MgFe}_2\text{Cl}_8(\text{g})$, $\log K = 4150/T - 4.59$ (885 K; transpiration, chemical transport); $\text{CaFe}_2\text{Cl}_8(\text{g})$, $\log K = 2660/T - 4.56$ (930 K; transpiration, chemical transport); $\text{SrFe}_2\text{Cl}_8(\text{g})$, $\log K \approx 2960/T - 4.51$ (1010 K; chemical transport); $\text{BaFe}_2\text{Cl}_8(\text{g})$, $\log K \approx 2250/T - 4.52$ (970 K; chemical transport); $\text{CoGa}_2\text{Cl}_8(\text{g})$, $\log K \approx 1860/T - 4.74$ (670 K; VIS spectroscopy); $\text{CoAl}_2\text{Br}_8(\text{g})$, $\log K = 3500/T - 4.79$ (610 K; transpiration, VIS spectroscopy); $\text{CuAl}_2\text{Cl}_8(\text{g})$, $\log K = 4450/T - 4.84$ (555 K; transpiration, VIS spectroscopy). The stability of gaseous complexes is discussed in terms of a simple thermodynamic model.

Introduction

During the last few years, there has been an increasing interest in gaseous complexes of metal halides (see ref 1-8 in ref 1). Most of the recent research has dealt with gaseous complexes formed between chlorides of bivalent metals and aluminium or ferric chloride as shown in reaction 1, where M

$$\text{MX}_2(\text{s}) + 2\text{LX}_3(\text{g}) \rightleftharpoons \text{ML}_2\text{X}_6(\text{g}) \quad (1)$$

= alkaline earth metal, transition metal; L = Fe, Al; X = Cl.

Because we were interested in stability trends, we investigated the formation of the following gaseous complexes: $\text{MgFe}_2\text{Cl}_8(\text{g})$, $\text{CaFe}_2\text{Cl}_8(\text{g})$, $\text{SrFe}_2\text{Cl}_8(\text{g})$, $\text{BaFe}_2\text{Cl}_8(\text{g})$, $\text{CoGa}_2\text{Cl}_8(\text{g})$, $\text{CoAl}_2\text{Br}_8(\text{g})$, $\text{CuAl}_2\text{Cl}_8(\text{g})$.

Methods and Computations

Chemicals. Anhydrous FeCl_3 , CoBr_2 , and MCl_2 (M = Mg, Ca, Sr, Ba) were prepared from analytical grade hydrated salts by standard procedures.² Commercial anhydrous AlCl_3 was purified by subliming it under dynamic vacuum from an AlCl_3 -charcoal mixture.³ Anhydrous GaCl_3 was supplied by courtesy of the Aluisse Co., Neuhausen, Switzerland.

Transpiration. The equilibrium constants of reaction 1 for the formation of $\text{MgFe}_2\text{Cl}_8(\text{g})$, $\text{CaFe}_2\text{Cl}_8(\text{g})$, and $\text{CuAl}_2\text{Cl}_8(\text{g})$ were measured by transpiration with equipment described elsewhere.^{13,14} A stream of argon or nitrogen first passed through solid LCl_3 (140-250 °C) and then through MgCl_2 (575-650 °C), CaCl_2 (600-715 °C), or CuCl_2 (230-330 °C). The salt vapors entrained with the inert gas were condensed upstream and the condensates were analyzed by atomic absorption or (and) chelatometry.

In the determination of the stability of $\text{CoAl}_2\text{Br}_8(\text{g})$, AlBr_3 was generated in situ by passing the inert gas first through liquid Br_2 at 0 °C and then through aluminum shot (450-550 °C).

The amount of inert carrier gas passing through the salts was measured with a calibrated gas meter and the flow rate was read from a Fisher-Porter flowmeter. In the range of flow rates used (approximately 7-80 $\text{cm}^3 \text{min}^{-1}$) the equilibrium constants of reaction 1 were independent of the flow rate, proving that equilibrium between flowing gases and $\text{MX}_2(\text{s})$ was established.

At the equilibrium temperature the volume V_{tot} of all the gases passing through the transpiration apparatus is

$$V_{\text{tot}} = V_{\text{carrier gas}} + V_{\text{L}_2\text{X}_6} + V_{\text{LX}_3} + V_{\text{complex}} + V_{\text{MX}_2} \quad (2)$$

The relative magnitudes of these volumes are

$$V_{\text{carrier}} \gg V_{\text{L}_2\text{X}_6} > V_{\text{LX}_3} > V_{\text{complex}} \gg V_{\text{MX}_2} \quad (3)$$

and consequently

$$V_{\text{tot}} \approx \left[n_{\text{carrier}} + \frac{n_{\text{L,tot}}}{2} \right] \frac{RT}{p_{\text{barom}}} \quad (4)$$

where n is the number of moles, $R = 0.08205 \text{ l. atm mol}^{-1} \text{ deg}^{-1}$, T is the equilibrium temperature (K), and p_{barom} is the atmospheric pressure ($0.923 \pm 0.013 \text{ atm}$). n_{carrier} is calculated from the measured volume of the carrier gas while $n_{\text{L,tot}}$ is obtained from the analysis of the entrained and afterward condensed L_2X_6 . The vapor pressure p_c of the gaseous complex follows from

$$p_c = \frac{n_{\text{MX}_2} RT}{V_{\text{tot}}} - p_{\text{MX}_2} \quad (5)$$

where n_{MX_2} is known from the analysis of the entrained MX_2 and p_{MX_2} is taken from the literature.^{4,5} In most of the experiments $p_c \gg p_{\text{MX}_2}$.

If the mass balance

$$n_{\text{LX}_3, \text{tot}} = 2n_{\text{L}_2\text{X}_6} + n_{\text{LX}_3} + 2n_{\text{ML}_2\text{X}_6} \quad (6)$$

is combined with the perfect gas law and with the dissociation equilibrium of $\text{L}_2\text{X}_6(\text{g})$ (Al_2Cl_6 ,⁶ Al_2Br_6 ,⁵ Fe_2Cl_6), eq 7 is obtained

$$p_{\text{LX}} = \frac{-K_{\text{diss}}}{4} + \left[\left(\frac{K_{\text{diss}}}{4} \right)^2 + \frac{K_{\text{diss}} n_{\text{L,tot}} p_{\text{barom}}}{2n_{\text{carrier}} + n_{\text{L,tot}}} - K_{\text{diss}} p_c \right] \quad (7)$$

which allows us to calculate p_{LX_3} .

As only a small fraction of the total amount of LX_3 is tied up in the complex, its stoichiometry, assumed to be ML_2X_6 in eq 6, has almost no effect on p_{LX_3} . Furthermore the system is buffered with